

cambridge.org/mrf

Ayman A. Althuwayb¹  and Divya Chaturvedi² 

¹Department of Electrical Engineering, College of Engineering, Jof University, Sakaka, Aljof 72388, Saudi Arabia and ²Department of Electronics and Communication Engineering, SRM University-AP, Mangalagiri, Andhra Pradesh 522 240, India

Research Paper

Cite this article: A. Althuwayb A, Chaturvedi D (2023). A triple-band dual-fed frequency-flexible SIW cavity-backed slot antenna. *International Journal of Microwave and Wireless Technologies* **15**, 282–288. <https://doi.org/10.1017/S1759078722000241>

Received: 14 March 2021
Revised: 1 February 2022
Accepted: 3 February 2022
First published online: 24 February 2022

Keywords:

Eight-mode substrate integrated waveguide (EMSIW); isolation; quarter-mode substrate integrated waveguide (QMSIW); triple-band antenna

Author for correspondence:

Ayman A. Althuwayb,
E-mail: aaalthuwayb@ju.edu.sa

Abstract

This article presents a novel dual-fed triple-frequency bands antenna using quarter-mode (QM)/ Eight-mode (EM) substrate integrated waveguide (SIW) cavity resonators. A V-shaped slot is etched into the patch to divide the half-mode cavity into one QM and two EM cavities. One section of the EM cavity and QM cavity are excited with the help of individual micro-strip feedlines. This configuration yields two distinct frequency bands at 4.85 GHz due to TE₁₁₀ mode of the EMSIW cavity and 5.87 GHz due to TE₁₁₀ mode of the QMSIW cavity confirming the self-diplexing property. Later, when both the EM cavity sections are joined with the help of two metallic strips, an additional resonance appears at 7.34 GHz due to the excitation of TE₁₂₀ mode. As compared to the conventional counterparts, the proposed structure is compact and simple. The footprint of the top patch is $0.6\lambda_1 \times 0.3\lambda_1$. To authenticate the proposed idea, the design is experimentally verified, and the measured results show a good covenant with the simulated results.

Introduction

In recent years, with the advancement of modern wireless communication, the demand for compact, low-profile multi-band antennas with better radiation characteristics has been increasing extensively. The cavity-backed antennas have fascinated researchers for a long decade with their high efficiency, gain, and unidirectional radiation characteristics. However, due to the use of the backed cavity, the overall thickness of the antenna becomes significantly higher which leads to a non-planar structure. In recent times, the substrate integrated waveguide (SIW) evolved as a promising technology to develop microwave passive components [1]. It has capability to offer waveguide like features such as high-quality factor and better power handling capability in a planar laminate. The SIW cavity adds the advantage of a simple printed circuit board (PCB) cost-efficient manufacturing process [2, 3].

As wireless technology has been becoming prominent, the need of multi-channels for the transceivers is conspicuous [4]. The transceivers on the same board suffer from the problem of poor isolation from the adjacent one [5]. The self-diplexing/triplexing antennas are in trends since they avoid the need for filtering feeding network, hence due to this reason the complexity of the overall system reduces significantly. The peculiar arrangement of the slots and the feed maintain good isolation in a compact and low-profile structure. In literature, the self-diplexing/triplexing SIW cavity-backed antennas are investigated to satisfy the requirement where multiple slots are excited by individual feedlines with maintaining adequate intrinsic isolation among the ports [5–20]. The individual excitation of slots avoids the need for decoupling elements in the feeding network which makes the overall structure compact and simple. In [6], a dual-polarized antenna is developed with enhanced isolation using a nested cavity-type arrangement. The self-diplexing antennas are developed by using a half-mode SIW resonator with an open-ended rectangular slot in [7–9]. The above-mentioned antenna provides average intrinsic isolation of 20 dB with dual frequency bands. However, in today's scenario with the demands of multi-channel communication, the need for transceivers more than dual frequency bands is increasing every day. To enhance the number of channels, a self-triplexing antenna is realized on a double-layered structure in [10], where better isolation is maintained among the adjacent elements by using BPF. In [11], a self-triplexing antenna is realized by exciting two bowtie slots using three feeds, provides average isolation of 22 dB with a relatively larger size. The antenna developed in [12] offers a relatively compact structure but a poor co-cross polarization ratio. In [13], two transverse slots and one annular rectangular slot are involved. The antenna geometry provides better isolation characteristics and a co-cross polarization ratio but relatively larger size. In order to achieve a compact structure, self-triplexing property is realized on a half-mode SIW cavity in [14]. The antenna offers compactness with poor isolation characteristics. The antenna developed in [15] offers better isolation but relatively poorer bandwidth. The above antennas are viable in terms of frequency tuning

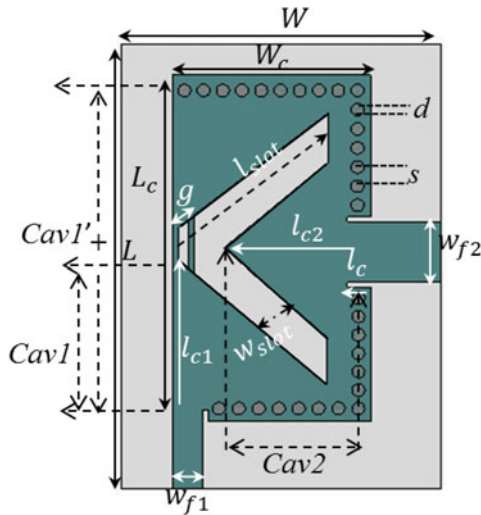


Fig. 1. Schematic diagram of proposed design, Dimensions ($W=25, L=36, L_c=26, W_c=13.5, l_{c1}=11, l_{c2}=10, l_{slot}=14.5, w_{slot}=4, g=0.85, d=1, s=2, w_{f1}=2.4, w_{f2}=4.8$) (Units: mm).

with different types of radiating slots and their combinations. However, the proposed antenna offers much simple and compact structure than any other existing self-triplexing antenna. Furthermore, many designs with good in-band performance were presented in [16–21].

In this paper, a novel technique for additional frequency band generation using metallic strips is projected. The proposed antenna is compact in size, provides triple frequency-band communication at 4.85, 5.87, and 7.3 GHz, respectively. Initially, a self-diplexing antenna is realized by etching a non-resonant V-shaped slot on the half-mode SIW cavity. Later, a self-triplexing antenna is designed by joining two EM-cavity sections. In self-diplexing configuration, the slot divides the half-mode cavity into two eight mode cavity sections and one quarter-mode (QM) cavity. The antenna yields dual-frequency bands, when one EM cavity and a QM cavity is fed with an individual microstrip feed line. On the other side, when the metallic strips are inserted to join the two EMSIW cavity sections, the antenna yield one more resonance due to the excitation of TE_{120} mode. Therefore, the triple frequency bands are achieved by inserting metallic strips in a V-shaped-slot dual-fed antenna configuration. The proposed geometry has the viability to use dual or triple frequency bands as per requirement. The organization of the paper is summarized as follows. First, a dual-frequency antenna is designed and investigated thoroughly. Second, a triple frequency band antenna is designed and optimized. In the next section, the experimental results of the fabricated prototype have been discussed and compared with the simulated results. The comparison of the proposed antenna with the other prevailing antennas is illustrated in the last section.

Design and principle of operation

The proposed HMSIW cavity-backed slot antenna configuration is exhibited in Fig. 1. The design evolution topology from the full-mode cavity to the miniaturized proposed antenna has been demonstrated in Fig. 2. All the simulations are carried out using CST 2018 Electromagnetic Simulator. Initially, the dimensions of the full

mode square SIW cavity is evaluated from (1) illustrated below [19].

$$f_{110(EM)} = \frac{c}{2\sqrt{\epsilon_{reff}}} \sqrt{\left(\frac{1}{W_{eff(EM)}}\right)^2 + \left(\frac{1}{L_{eff(EM)}}\right)^2} \tag{1}$$

for QMSIW cavity

$$f_{110(QM)} = \frac{c}{2\sqrt{\epsilon_{reff}}} \sqrt{\left(\frac{1}{2W_{eff(QM)}}\right)^2 + \left(\frac{1}{2L_{eff(QM)}}\right)^2} \tag{2}$$

for EMSIW cavity

$$f_{110(EM)} = \frac{c}{2\sqrt{\epsilon_{reff}}} \sqrt{\left(\frac{1}{2W_{eff(EM)}}\right)^2 + \left(\frac{1}{4L_{eff(EM)}}\right)^2} \tag{3}$$

W_{eff} and L_{eff} are the effective width and length and of the cavity where $W_{eff} = W_c - (d^2/0.95s)$, $L_{eff} = L_c - (d^2/0.95s)$,

$$\epsilon_{reff} = \left(\frac{\epsilon_r+1}{2}\right) + \left(\frac{\epsilon_r-1}{2}\right) \frac{1}{\sqrt{1+(12h/w_f)}}$$

where ϵ_{reff} is the effective dielectric constant, ϵ_r is the dielectric constant of the material, w_f is the trace thickness, d is the diameter and s is the spacing between vias, W_c, L_c are the physical width and length of the cavity. The sidewalls of the square SIW cavity are formed by embedding the shorting vias to connect the top and bottom metallic claddings. The cavity is fed with two 50 Ω microstrip feed lines into two orthogonal planes, shown in Fig. 2(a). The TE_{110} mode of the FMSIW cavity resonates at 5.3 GHz. Due to the symmetrical nature of the dominant mode, a half-mode cavity is realized by bisecting it along one of the magnetic walls, shown in Fig. 2(b).

The half- TE_{110} mode shifts toward the lower frequency side and resonates at 5 GHz. This downward shift is obtained due to an increment in the fringing field from the open side of the cavity. To achieve a self-diplexing antenna property, a non-resonant V-shaped slot of one side length (l_{slot}) $0.65\lambda_g$ is etched on the top wall of the HMSIW cavity. The slot divides the HMSIW cavity into two EMSIW and one QMSIW cavity. This arrangement of hybrid cavity resonators yields two distinct resonances at 4.85 and 5.87 GHz, respectively when one EMSIW and QMSIW fed with separate microstrip feedlines. Both the cavities predominantly radiate through the V-shaped slot due to the modified TE_{110} modes of their respective cavities. The dimensions of the QM/EM cavities can be evaluated from (2) & (3) [4]. The leakage of power from one port to another port is minimal due to the orthogonal polarization of the field from both cavities. The isolation is maintained up to 32 dB that is better than almost any of the existing antennas in the literature [6–14]. The return loss can be improved easily by altering the feed-line dimensions i.e. l_c, w_{f1} and w_{f2} .

Results and discussions

The proposed triple-frequency band antenna is formed by joining the two EMSIW cavity sections with the help of two metallic strips. The proposed antenna produces three distinct resonances at 4.85 GHz, 7.3 GHz due to $Cav1'$ and at 5.85 GHz due to $Cav2$. The overall footprint of the proposed antenna is $0.57\lambda_1 \times 0.8\lambda_1$ mm². The design steps and parametric analysis are explained in a more detailed way in the preceding sections.

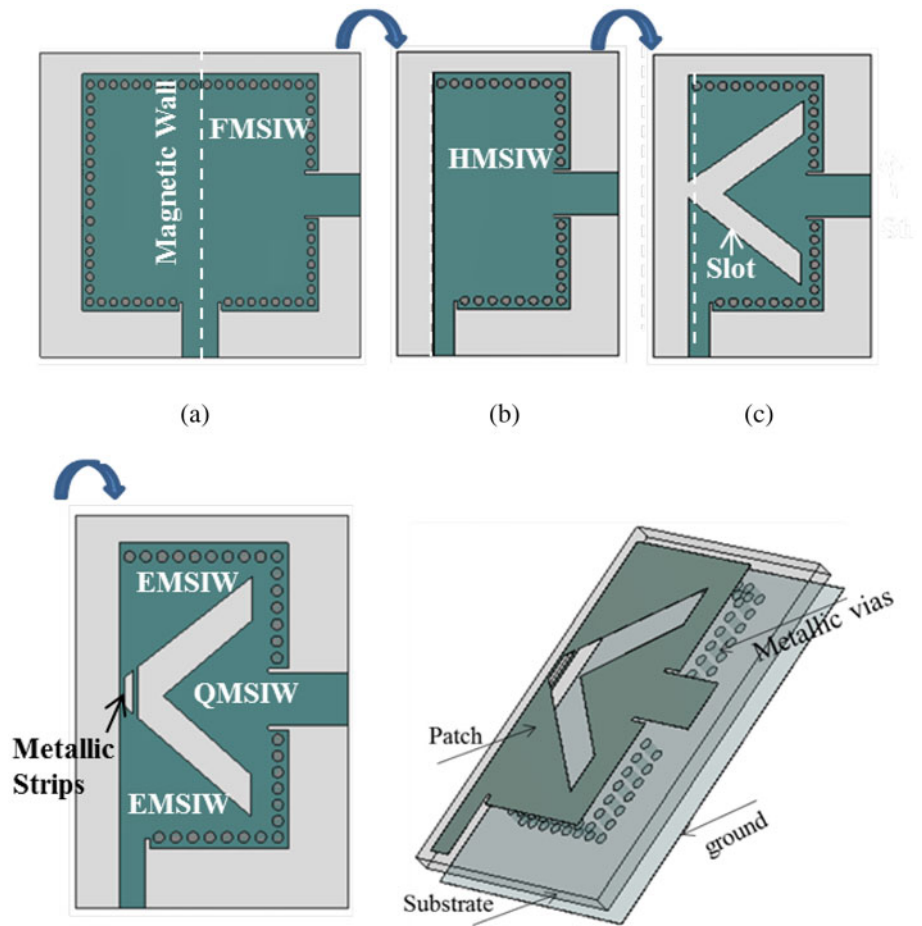


Fig. 2. Construction of proposed triple-band antenna: (a) FMSIW cavity (b) HMSIW cavity (c) combination of hybrid cavity resonators (2EMSIW + QMSIW) (d) proposed antenna geometry (e) perspective view of the proposed antenna.

Self-Diplexing antenna

Without metallic strips, the *Cav1* is an original EMSIW cavity. To achieve a compact size self-diplexing antenna, TE_{110} mode is selected as an operating mode for both cavities. EMSIW cavity is fed with half of the width of the 50Ω characteristic impedance line to match with the cavity input impedance. Thus, the feed width is optimized to cancel the imaginary impedance and to achieve better impedance matching. Port decoupling is accomplished better than 30 dB due to orthogonal polarization of the fields as well as the large width (w_{slot}) of the slot. The electric field distributions in both the cavities are displayed in Fig. 3. When *Port1* is ON, the field primarily radiates through the slot and some portion from the open sidewall. On the other hand, when *Port2* is ON, the total field radiates through the slot with maintaining a good decoupling with the other port. The distinct resonances appear at 4.85 and 5.87 GHz due to unequal perturbation of the fields by the slot, shown in Fig. 4. The length of the slot plays a key role in improving the isolation as well as tuning both the resonant frequencies. As the length of the slot increases, both the frequency bands shift downward due to an increment in the length of the cavities.

Also, the isolation between ports is getting improved substantially due to a decrease in the aperture that enhances the coupling between the corner sides of the cavities, the same can be observed from Fig. 5. Besides the slot length, both the resonances further can be tuned in the desired frequency range by varying the cavity lengths. It can be observed from Fig. 6(a), when the length of the cavity l_{c1} increases in the range of 11–12.5 mm, the resonant

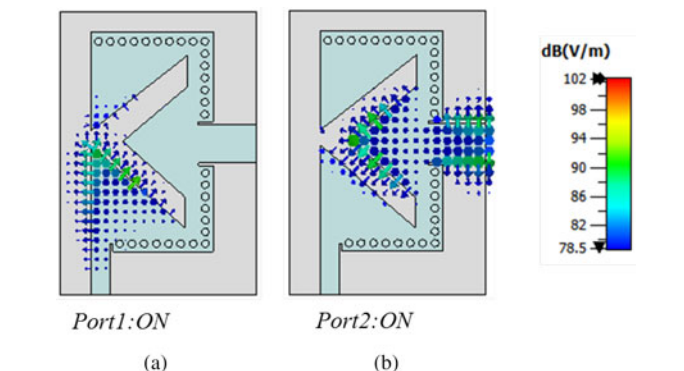


Fig. 3. Electric field vector at top metallic plane: (a) TE_{110} mode at 4.85 GHz (*Port1*: ON) (b) TE_{110} mode at 5.87 GHz (*Port2*: ON).

frequency correspondingly decreases from 5.3 to 4.8 GHz. Similar behavior can be observed in Fig. 6(b), as the l_{c2} increases in the range of 9.5–11 mm, the corresponding resonant frequency decreases 6.25–5.8 GHz. Hence, it can be concluded that both resonances have great flexibility of tuning along with maintaining a better decoupling between the ports.

Proposed geometry: self-diplexing antenna with metallic strips

The triple-band antenna is realized by inserting two metallic strips that join the EMSIW cavities to form *Cav1'*. Thus, three resonating sections are combined to arrive at a miniaturized

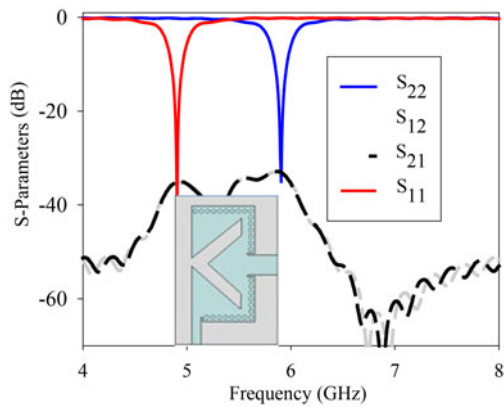


Fig. 4. Simulated S-parameters of the self-dixing antenna.

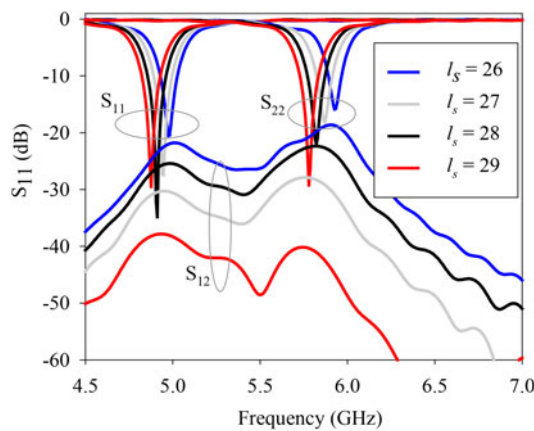


Fig. 5. Simulated S-parameters vs frequency with different lengths of the slot.

antenna. With the effect of insertion of the strips, the boundary conditions for the existence of TE_{120} mode get satisfied and the corresponding resonance appears at 7.34 GHz. However, the TE_{110} mode of the original EMSIW cavity ($Cav1$) does not get disturbed from its position because the EMSIW cavities consist of symmetrical field distribution. The S-parameters after introducing the strips in the self-dixing antenna have been exhibited in Fig. 7. From the S_{21} plot, it can be observed that the port decoupling does not get disturbed with the inclusion of the strips. The vector electric field distribution for each resonance frequency is displayed in Fig. 8. The first resonance with $Port1$ excitation displays the field distribution in the same phase in both EMSIW cavities, confirms TE_{110} mode existence. Also, another resonance due to $Port1$ excitation shows equal and opposite phase in the combination of EMSIW cavities confirms the TE_{120} mode. The resonance with $Port2$ excitation confirms TE_{110} in the QMSIW cavity. It can be observed from the simulated reflection coefficient plot that after introducing the strips, the bandwidth of first resonance (i.e. $Cav1'$) is getting decreased than the TE_{110} mode of the $Cav1$ [16, 17]. Without the strips, the whole energy is confined in one TE_{110} mode. However, after inserting the strips the same energy is distributed between two modes i.e. TE_{110} and TE_{120} . Thus, both the modes become mutually dependent on each other. An additional strip is introduced with the main strip for better impedance matching at both the resonances, which can be observed in Fig. 9. As the gap between the two strips increases, the first resonance shifts downward while the third resonance shifts upward.

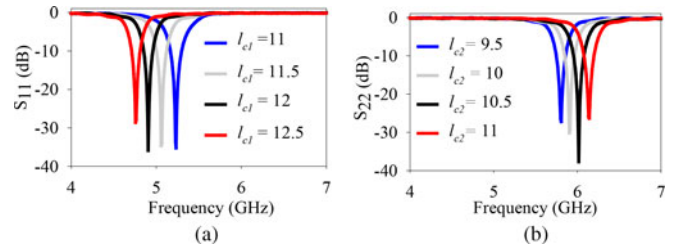


Fig. 6. Simulated S-parameters with different cavity lengths (a) S_{11} vs frequency for various l_{c1} and (b) S_{22} vs frequency for various l_{c2} .

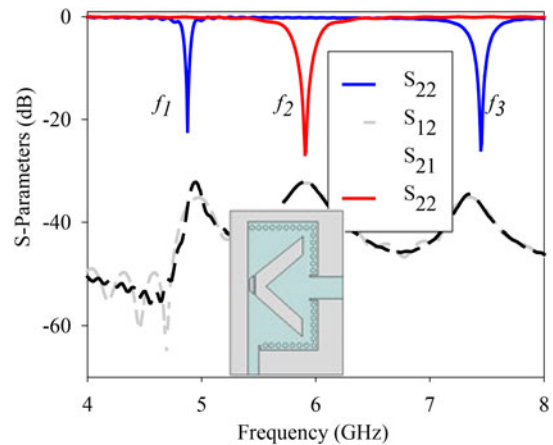


Fig. 7. Simulated S-parameters of the self-dixing antenna without strips.

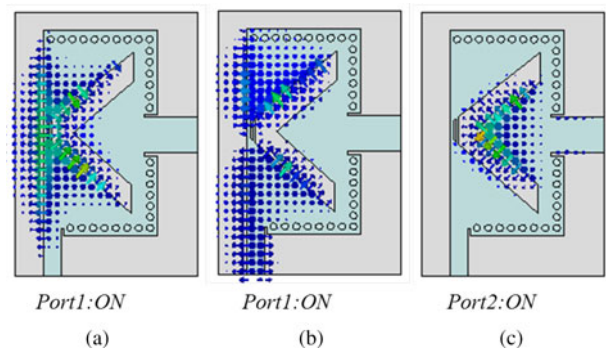


Fig. 8. Electric field vector at dielectric surface: (a) TE_{110} mode at 4.85 GHz ($Port1$: ON) (b) TE_{120} mode at 7.3 GHz ($Port1$: ON) TE_{110} mode at 5.85 GHz ($Port2$: ON).

For the first resonance, the TE_{110} mode is maximally concentrated at the center of the strips. While the third resonance belongs to TE_{120} mode consists of a minimum field at the center of strips.

Thus, when the gap g increasing, the effective width of the radiating strips also increasing, which leads to a decrease in the resonant frequency for the first mode. For the TE_{120} mode, the impedance matching is getting improved, and frequency shifts upward because of a decrease in the series capacitance [17]. Also, the intrinsic isolation between the ports improves with g parameter. From the parametric variation, it can be observed that the antenna design is flexible in terms of tuning frequencies (i.e. f_1, f_2, f_3) with respect to parameters (l_s, l_{c1}, l_{c2} , and g). The optimized dimensions after parametric variations are displayed in the caption of Fig. 1.

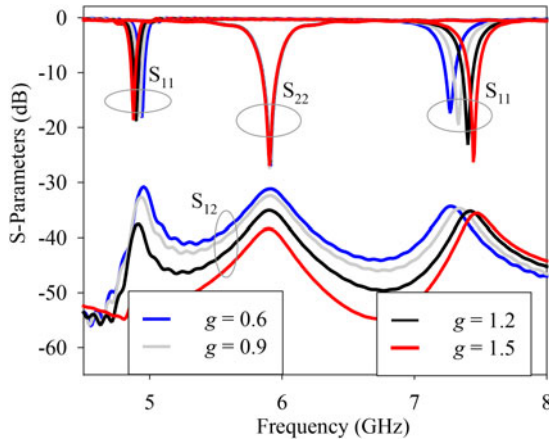


Fig. 9. S-parameters vs frequency for different gap between the strips.

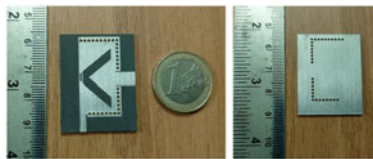


Fig. 10. Fabricated prototype of the proposed antenna geometry.

Design Guidelines:

- A square SIW cavity of size $0.57\lambda_1 \times 0.8\lambda_1 \text{ mm}^2$ is designed using (1)
- To obtain the miniaturization, a half-mode SIW cavity is realized by bisecting the full-mode cavity along one of the magnetic walls.
- A non-resonant V-shaped slot is etched on the top-plane of HMSIW cavity to accomplish two EM and QM SIW cavity sections.
- The dimensions of the EMSIW and QMSIW cavities are determined from (2) & (3).
- A self-diplexing property is accomplished by individually exciting one EMSIW and QMSIW cavity sections.
- Two strips are inserted to yield one additional resonance due to the TE_{120} mode of the $Cav1'$.
- The resonances can be tuned in a range of frequencies by varying the l_{slot} , l_{c1} , l_{c2} .

Experimental validation

A prototype of the proposed geometry is fabricated using a Rogers 5880 substrate laminate of thickness 1.57 mm and loss-tangent 0.0009.

The proposed triple-band antenna is experimentally verified in terms of S-parameters, gain, and 2D-radiation patterns. The measurements are performed using MS46122B Vector Network Analyzer. The fabricated prototype of the proposed antenna configuration is depicted in Fig. 10. When $Port1$ is excited, the antenna produces simulated frequency resonances at 4.85 and 7.35 GHz. On the other hand, when $Port2$ is excited, the antenna shows resonance at 5.85 GHz.

The antenna shows the measured results at 4.75 and 7.27 GHz when $Port1$ is fed and $Port2$ is terminated with the matched load.

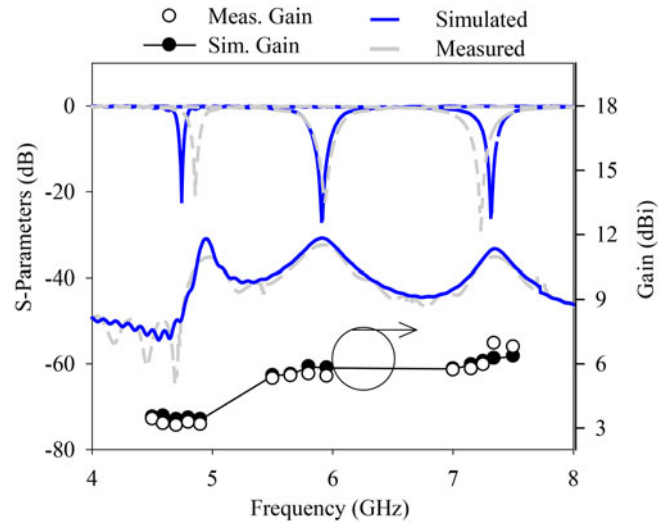


Fig. 11. Simulated and measured S-parameters, gain vs frequency.

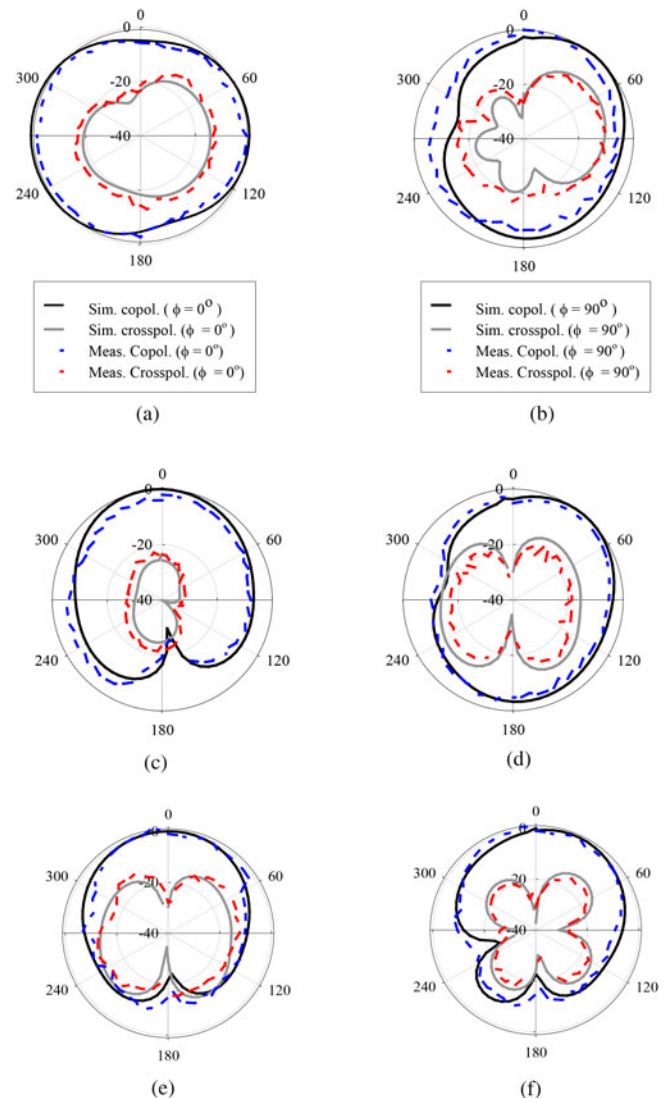


Fig. 12. Simulated and measured radiation patterns for E-plane ($\phi = 0^\circ$) and H-plane ($\phi = 90^\circ$) (a), (b) at 4.75 GHz (c), (d) at 5.9 GHz, and (e), (f) at 7.27 GHz.

Table 1. Comparison of proposed work with the other existing works

Param.	fr (GHz)	Gain (dBi)	FTBR (dB)	Isolation (dB)/No. of ports	Size in (Electrical length)
[10]	0.85	0.85	N.A.	>19 /3	$0.53 \lambda_1 \times 0.36 \lambda_1$
	1.65	4			
	2.45	4.23			
[11]	7.89	7.2	>17.3	22.5/3	$1.3 \lambda_1 \times 1.3 \lambda_1$
	9.44	7.2			
	9.87	7.2			
[12]	6.5	3.68	>13	18 / 3	$1.0\lambda_1 \times 1.0 \lambda_1$
	7.6	4.76			
	9	4.5			
[13]	4.2	6.56	>19	23 / 3	$1.2\lambda_1 \times 0.9 \lambda_1$
	5.2	4.2			
	5.8	5.85			
[14]	4.95	4.5	>14	20.5/3	$0.3 \lambda_1 \times 0.63 \lambda_1$
	5.3	4.9			
	5.9	6.1			
[15]	4.14	4.26	>15	28.4 / 3	$0.45\lambda_1 \times 0.45 \lambda_1$
	6.1	4.41			
	8.32	6.27			
[20]	5.57	4.10	>13	>21.3	$0.67\lambda_1 \times 0.65\lambda_1$
	7.17	3.95			
	7.65	3.54			
[21]	5.54	4.48	N.A.	>24.1	$0.86\lambda_1 \times 0.86\lambda_1$
	6.61	3.70			
	6.67	4.3			
This work	4.85	3.3	>14	32/2	$0.3\lambda_1 \times 0.6 \lambda_1$
	5.85	5.6			
	7.3	5.9			

* λ_1 is the guiding wavelength at first resonance frequency, N.A.* (not available).

Similarly, it produces resonance at 5.9 GHz when *Port2* is fed and *Port1* is terminated with the matched load, shown in Fig. 11. The antenna produces the simulated values of gain 3.5, 5.5, and 6.2 dBi and measured values of gain 3.3, 5.6, and 5.9 dBi at 4.75, 5.9, and 7.27 GHz, respectively. There is a minor discrepancy is observed in the simulated and measured values of gains due to the insertion loss of the connectors and cables. The normalized radiation characteristic of the antenna is measured at two principle cut planes at ($\phi = 0^\circ$) and ($\phi = 90^\circ$) and plotted in Fig. 12 at each resonant frequency. The overall front-to-back ratio is better than 15 dB for E-plane ($\phi = 0^\circ$) and around 10 dB for H-plane ($\phi = 90^\circ$). The cross-polar levels are at least 20 dB lower than the co-polar level at each resonant frequency, specifically in the bore-sight direction. To show the best part of the design, the performance of the proposed triple-band dual-fed antenna is compared with other reported works [10–15, 20, 21] in Table 1. It can be observed that the proposed solution is more compact with moderate values of gain and a uniform radiation pattern. The proposed antenna is viable to use for dual/triple frequency band

operations depending upon the usage of metallic strips. Moreover, the proposed antenna can be scaled in the desired frequency band by varying the dimensions of the cavities and slot.

Conclusion

This article presents a compact, low profile SIW cavity-backed slot antenna for dual/triple band operations depending on the usage of metallic strips. The antenna is novel in the operation as with the incorporation of metallic strips, an additional resonance starts appearing at 7.35 GHz without disturbing the resonances of the original EM and QM cavities of the self-diplexing antenna. The antenna structure radiates through a V-shaped slot with better intrinsic isolation between the ports than any other existing self-triplexing antenna developed in recent times. The experimental results validate a good matching with simulation counterparts. Moreover, the proposed design offers the advantages of the low-profile slot antenna and the planar cavity to attain moderate gain, unidirectional radiation performance in a highly compact

size. The presented geometry shows better isolation and more compacted size than any other work available in the literature. In future work, a diode can be used as a switch in the place of metallic strips to enhance flexibility in the electrically tuning of the circuit.

Acknowledgements. This work was funded by the Deanship of Scientific Research at Jouf University under grant No (DSR-2021-02-0388)

References

1. **Kumar A and Althuwayb AA** (2021) SIW resonator based duplex filter. *IEEE Antennas and Wireless Propagation Letters* **20**, 2544–2548.
2. **Luo GQ, Hu ZF, Dong LX and Sun LL** (2008) Planar slot antenna backed by substrate integrated waveguide cavity. *IEEE Antennas and Wireless Propagation Letters* **7**, 236–239.
3. **Chaturvedi D** (2020) SIW cavity-backed 24° inclined-slots antenna for ISM band application. *International Journal of RF and Microwave Computer-Aided Engineering* **30**, e22160.
4. **Deckmyn T, Agneessens S, Reniers AC, Smolders AB, Cauwe M, Ginste DV and Rogier H** (2017) A novel 60 GHz wideband coupled half-mode/quarter-mode substrate integrated waveguide antenna. *IEEE Transactions on Antennas and Propagation* **65**, 6915–6926.
5. **Hao Y and Painsi CG** (2002) Isolation enhancement of anisotropic UC-PBG microstrip diplexer patch antenna. *IEEE Antennas and Wireless Propagation Letters* **1**, 135–137.
6. **Chaturvedi D, Kumar A and Raghavan S** (2019) A nested SIW cavity-backing antenna for Wi-Fi/ISM band applications". *IEEE Transactions on Antennas and Propagation* **67**, 2775–2780.
7. **Kumar A, Chaturvedi D and Raghavan S** (2019) Dual-band, dual-fed self-diplexing antenna. *2019 13th European Conference on Antennas and Propagation (EuCAP)*, 31 Mar 2019, pp. 1–5.
8. **Kumar A, Chaturvedi D and Raghavan S** (2018) Design of a self-diplexing antenna using SIW technique with high isolation. *AEU-International Journal of Electronics and Communications* **94**, 386–91.
9. **Kumar A, Chaturvedi D and Raghavan S** (2019) Design and experimental verification of dual-fed, self-diplexed cavity-backed slot antenna using HMSIW technique. *IET Microwaves, Antennas & Propagation* **13**, 380–385.
10. **Cheong P, Chang KF, Choi WW and Tam KW** (2015) A highly integrated antenna-triplexer with simultaneous three-port isolations based on multi-mode excitation. *IEEE Transactions on Antennas and Propagation* **63**, 363–368.
11. **Kumar K and Dwari S** (2017) Substrate integrated waveguide cavity-backed self-triplexing slot antenna. *IEEE Antennas and Wireless Propagation Letters* **16**, 3249–3252.
12. **Arvind K and Singaravelu R** (2018) Self-triplexing SIW cavity-backed slot antenna. *IEEE Antennas and Wireless Propagation Letters* **17**, 772–775.
13. **Chaturvedi D, Kumar A and Raghavan S** (2018) An integrated SIW cavity-backed slot antenna-triplexer. *IEEE Antennas and Wireless Propagation Letters* **17**, 1557–1560.
14. **Priya S and Dwari S** (2020) A compact self-triplexing antenna using HMSIW cavity. *IEEE Antennas and Wireless Propagation Letters* **19**, 1–5.
15. **Dash SK, Cheng QS, Barik RK, Pradhan NC and Subramanian KS** (2020) A compact triple-fed high-isolation SIW-based self-triplexing antenna. *IEEE Antennas and Wireless Propagation Letters* **19**, 766–770.
16. **Priya S, Dwari S, Kumar K and Mandal MK** (2019) Compact self-quadruplexing SIW cavity-backed slot antenna. *IEEE Transactions on Antennas and Propagation* **67**, 6656–6660.
17. **Kumar A and Raghavan S** (2016) A design of miniaturized half-mode SIW cavity-backed antenna. *2016 IEEE Indian Antenna Week (IAW 2016)*; IEEE, 6 Jun 2016, pp. 4–7. doi: 10.1109/IndianAW.2016.7883585
18. **Althuwayb AA, Al-Hasan MA, Kumar A and Chaturvedi D** (2021) Design of half-mode substrate integrated cavity inspired dual-band antenna. *International Journal of RF and Microwave Computer-Aided Engineering* **31**, e22520.
19. **Kumar A** (2020) Wideband circular cavity-backed slot antenna with conical radiation patterns. *Microwave and Optical Technology Letters* **62**, 2390–237.
20. **Kumar A and Raghavan S** (2018) Design of SIW cavity-backed self-triplexing antenna. *Electronics Letters* **54**, 611–612.
21. **Kumar A, Chaturvedi D, Saravanakumar M and Raghavan S** (2018) SIW cavity-backed self-triplexing antenna with T-shaped slot. *2018 Asia-Pacific Microwave Conference (APMC)*, 6 Nov 2018, pp. 1588–1590.



Ayman A. Althuwayb received the B. Sc. degree (Hons.) in electrical engineering (electronics and communications) from Jouf University, Saudi Arabia, the M.Sc. degree in electrical engineering from California State University, Fullerton, CA, USA, in 2015, and the PhD degree in electrical engineering from Southern Methodist University, Dallas, TX, USA, in 2018. He is currently an assistant professor

with the department of electrical engineering at Jouf University, Kingdom of Saudi Arabia. His current research interests include antenna design and propagation, microwaves and millimeter waves, wireless power transfer, ultrawideband and multiband antennas, filters and other.



Divya Chaturvedi received B.Tech. degree in electronics and communication engineering from Uttar Pradesh Technical University, India and M. Tech. in electronics engineering from Pondicherry Central University, India. She completed her doctorate degree in the Department of Electronics and Communication Engineering, National Institute of Technology Trichy (NIT-T) in 2019. Currently, she is an assistant

professor in SRM University AP, India.